

# UCSF

## UC San Francisco Previously Published Works

### Title

Mediator 1 contributes to enamel mineralization as a coactivator for Notch1 signaling and stimulates transcription of the alkaline phosphatase gene.

### Permalink

<https://escholarship.org/uc/item/6nj8z63f>

### Journal

The Journal of biological chemistry, 292(33)

### ISSN

0021-9258

### Authors

Yoshizaki, Keigo  
Hu, Lizhi  
Nguyen, Thai  
et al.

### Publication Date

2017-08-01

### DOI

10.1074/jbc.m117.780866

Peer reviewed



## Med1 activates alkaline phosphatase gene transcription

and ameloblasts during dental epithelial differentiation (7). Previous studies have indicated that Notch signaling facilitates differentiation of the dental epithelial cell line HAT-7 into *Alpl*-expressing SI-like cells *in vitro* (8). Notch signaling also plays a role in enamel mineralization, as *Jag2*-deficient mice display enamel hypoplasia (9).

Notch signaling is activated by cleavage of the intracellular domain of Notch receptors through  $\gamma$ -secretase. The intracellular domain of Notch moves to the nucleus and activates the transcription of target genes such as the hairy enhancer of split homologues-1 (*Hes1*) through the interaction of transcription factors such as the recombining binding protein suppressor of hairless (RBP-Jk). The transcription of target genes is promoted by the binding of the c-Notch–RBP-Jk complex to the RBP-Jk DNA-binding sites on their promoter. Notch1 signaling is activated by the overexpression of the Notch1 intracellular domain (NICD) or by chelating reagents such as EDTA through prevention of calcium-dependent dimerization of Notch proteins (10). In addition, the  $\gamma$ -secretase inhibitor DAPT inhibits Notch signaling by preventing the cleavage of Notch receptors. The transcription of Notch–RBP-Jk is activated by mastermind-like proteins, but the role of the transcriptional coactivator Mediator is not known, at least in mammalian systems.

Mediator is a multiprotein complex that facilitates transcription by bridging transcription factors and the RNA polymerase (pol II) transcriptional machinery. Mediator not only facilitates transcription in general but also controls the differentiation of a variety of cells by regulating fate-specific transcription factors (11–16). Mediator 1 (MED1) is one of the critical subunits for the Mediator complex (12), and the ablation of *Med1* causes abnormalities in cell differentiation of a number of cell types, including hematopoietic cells (17, 18), luminal cells (19, 20), and epidermal keratinocytes (21, 22). We generated conditional knock-out (KO) mice, in which *Med1* is removed from keratin 14 (*Krt14*)-expressing epithelia, and used these mice to show that *Med1* ablation causes defects in hair differentiation leading to alopecia in the skin (23). The same conditional *Med1* KO mice, in which *Med1* was also removed from *Krt14*-expressing dental epithelia, showed disruption in the development of incisors (24). *Med1* deletion causes defects in cell fate of incisor-specific adult stem cells, resulting in ectopic hair formation in the SI while reducing mineralization of the incisor enamel. Here, we investigated the role of MED1 in enamel mineralization using *Med1* KO molars in which hair was not generated but enamel mineralization was inhibited. We analyzed *Med1* KO molars at the secretory stage (P7) and found changes in Notch signaling and SI differentiation in *Med1* KO molars *in vivo*. These results led us to investigate the molecular mechanisms by which MED1 regulates Notch signaling and *Alpl* expression. We utilized the immortalized dental epithelial cell line SF2 that is derived from rat incisor and is capable of differentiating into the SI lineage (25, 26). We determined the impact of the overexpression or silencing of *Med1* on Notch1-regulated SI differentiation and on *Alpl* gene transcription. Our study demonstrates that MED1 promotes SI differentiation and activates the gene transcription of *Alpl* via Notch signaling, which is required for enamel matrix mineralization.

## Results

### *Med1* deficiency in dental epithelia causes defects in enamel matrix mineralization

Previously, we reported that *Med1* KO mice develop ectopic hair formation and hypomineralization of incisor enamel (24). Here, we re-evaluated the impact of *Med1* deletion on molar enamel mineralization. Ten-week-old floxed *Med1* mice containing the *Krt14Cre* transgene (KO) were compared with control (CON) littermates that had floxed *Med1* alleles but no *Cre*. *Med1* was removed from dental epithelial cells in *Med1* KO teeth, as shown in our previous study (24). The *Krt14Cre* transgene is expressed in all dental epithelia cell lineages in the developing tooth (27). A stereomicroscopic analysis of molars and incisors of CON mice showed translucent enamel but less of it in *Med1* KO molars (Fig. 1A). Moreover, the cusps of the KO molars and the tips of the KO incisors were rounded (Fig. 1A), suggesting increased wear. Microradiographic imaging of KO incisors showed an impaired calcified structure as compared with CON incisors (Fig. 1B, left panel). A micro-CT-scan of CON molars showed a thick radio-opaque enamel layer over dentin, whereas KO molars had a flat occlusal plane, likely due to attrition, with a marked decrease in the thickness of the enamel covering the dentin (Fig. 1B, right panel). Scanning electron microscopic analysis of CON incisors revealed highly organized enamel crystals over dentin, whereas the *Med1* KO incisors almost completely lacked these crystals (Fig. 1C). H&E staining indicated that KO incisors lacked a mineralized layer, although the matrix of the enamel layer was intact (Fig. 1D). These results indicate that enamel matrix mineralization is inhibited in *Med1* KO teeth, whereas enamel matrix proteins are present.

### *Med1* ablation specifically reduced *Alpl* expression in the SI layer but did not affect enamel matrix protein expression in ameloblasts

First, we evaluated the impact of *Med1* ablation on the differentiation of dental epithelial cells by examining the molars at P7. The molars were dissected from *Med1* KO and CON mice, and dental epithelial tissues were separated from mesenchymal tissues. RNA was isolated from epithelial tissues, and the mRNA levels of the KO epithelia were compared with those of CON epithelia using qPCR (Fig. 2A). The expression levels of the enamel matrix proteins secreted by ameloblasts, including *Amel*, *Ambn*, *Enam*, and matrix metalloproteinase-20 (*Mmp20*) were similar in the KO and CON molars. The levels of *Calb1*, a calcium-binding protein that is abundant in the maturation stage of ameloblasts, were also similar (Fig. 2A). However, mRNA levels of *Alpl*, which is specifically expressed in the SI layer, were down-regulated in *Med1* KO molars compared with CON molars (Fig. 2A). The protein levels of AMBN, AMEL, and ALPL in *Med1* KO and CON molars (P7) were evaluated by immunostaining (Fig. 2B). Both AMEL and AMBN were similarly deposited in the enamel matrix layer of the KO and CON molars (Fig. 2B). However, the relative immunostaining of the SI marker, ALPL, detected in the SI layer adjacent to the ameloblasts, was significantly reduced in the KO molars as compared with the CON molars (Fig. 2B). The analyses of both mRNA and

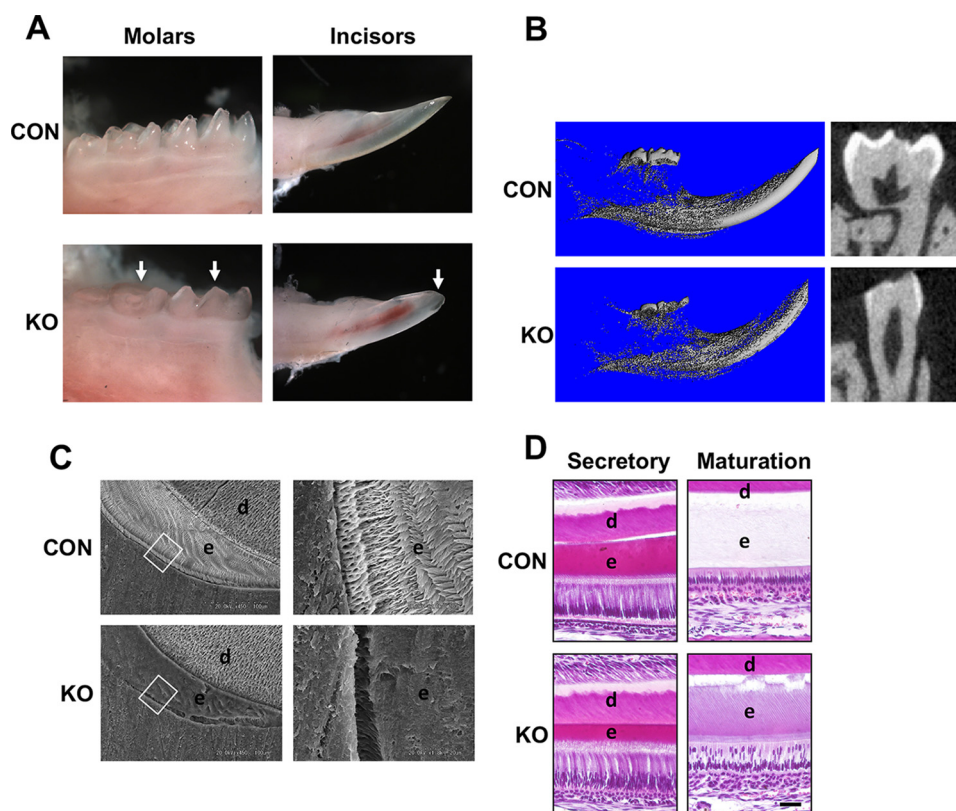


**Figure 1. Med1 deficiency in dental epithelia results in enamel hypoplasia in Med1 KO mice.** Molars and incisors of 10-week-old Med1 KO mice were compared with those of littermate CON mice. *A*, Med1 KO molars show rounded cusps, and Med1 KO incisors show rounded tips (arrows). *B*, MicroCT analysis of incisors (left panel) and molars (right panel). *C*, scanning electron microscope analysis of incisors. Enlarged images of the boxed areas are shown on the right panel. *D*, H&E staining of incisor sections at the secretory (left panel) and at the maturation stages (right panel). The incisors were first decalcified and processed. The CON section shows a blank area (e) indicating where the mineral in the enamel had been present before decalcification. In contrast, Med1 KO incisors still retained the enamel matrix layer but lacked a mineralized layer. Scale bars, 20  $\mu$ m; e, enamel matrix layer; d, dentin matrix layer or dentin (maturation).

protein indicated that Med1 ablation impairs SI differentiation but does not affect ameloblast differentiation, as indicated by the relatively normal levels of enamel matrix proteins.

#### Notch signaling is down-regulated in Med1 KO dental epithelial cells

Because Notch1 is expressed in SI cells, NOTCH1 and its signaling may regulate SI cell differentiation, resulting in Alpl induction. To test this possibility, we examined the expression levels of Notch receptors (Notch1 and Notch2) and Notch ligands (Jag1 and Jag2) and its target gene, Hes1, by qPCR using mRNA from dental epithelial tissues dissected from P7 molars of Med1 KO and CON mice (Fig. 3). qPCR analyses showed that mRNA levels of Notch1 and Hes1 were down-regulated in KO molars compared with CON molars (Fig. 3A). In contrast, the levels of Notch2 and Jag1 were not changed, and the decrease in Jag2 was not statistically significant (Fig. 3A). Immunostaining showed that NOTCH1 protein was also down-regulated in KO molars at P7 compared with CON molars, where NOTCH1 was specifically expressed in the SI layer but not in ameloblasts (Fig. 3B, left panels). The active form of Notch1, NICD, was also reduced in KO molars at P7 compared with CON molars, where it was exclusively detected in the nucleus of SI cells (Fig. 3B, right panels). In contrast, the localization and expression levels of NOTCH2, JAG1, and JAG2 proteins did not change in Med1 KO molars compared with CON molars (Fig. 3C). These results

demonstrated that the ablation of Med1 Notch1 signaling in SI cells by reducing Notch1 expression and activation.

#### Med1 regulates Alpl expression and Notch signaling in SF2 cells

The role of MED1 in SI differentiation and Notch signaling was examined using the dental epithelial cell line SF2. SF2 cells differentiate into the SI lineage, as indicated by the increased expression of Alpl with time in culture (Fig. 4A, left panel, vector control (Vec)). When Med1 was overexpressed, Med1 expression increased more than 50-fold (Fig. 4A, right panel (Med1)), and Alpl was further induced at the 96-h time point (Fig. 4A, left panel). When Med1 was silenced by siRNA (siMed1), Med1 was efficiently down-regulated compared with cells transfected with control siRNA (siCON) (Fig. 4B right panel), and the induction of Alpl expression was reduced (Fig. 4B, left panel). Med1 silencing also reduced the mRNA expression levels of Notch1 and Hes1 at 96 h (Fig. 4C). Med1 overexpression increased the protein level of NICD (Fig. 4D, left panel), although total NOTCH1 did not change (Fig. 4D). Med1 silencing (siMed1) reduced NICD but did not change total NOTCH1 (Fig. 4D, right panel). When SF2 cells were treated with EDTA, Notch signaling was activated, as shown by the increased levels of NICD, in a time-dependent manner (Fig. 4E). However, Med1 silencing by siMed1 delayed the increase in NICD levels with EDTA treatment (Fig. 4E). These results

## Med1 activates alkaline phosphatase gene transcription

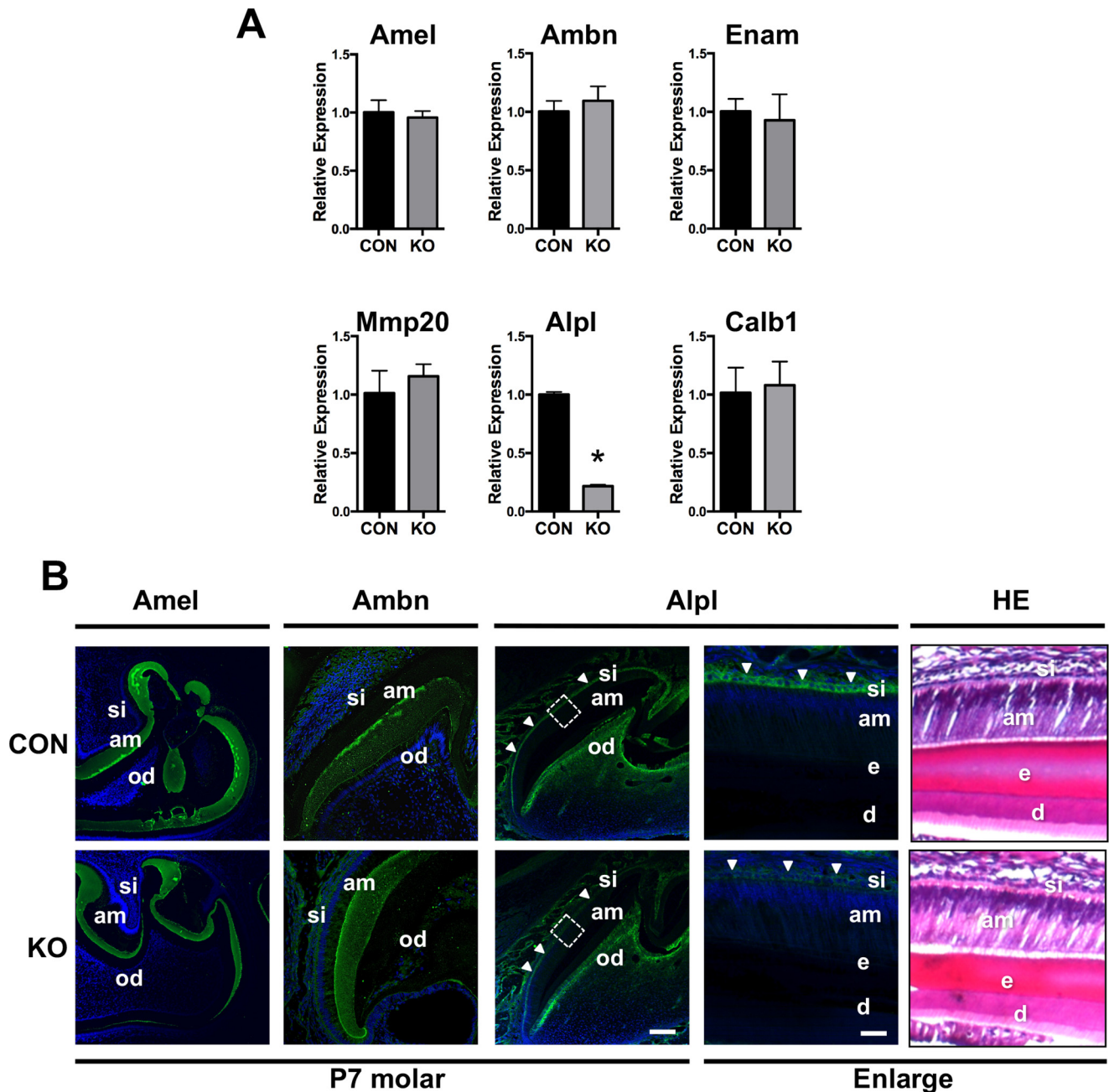


**Figure 2.** *Alpl* expression is down-regulated in dental epithelial tissues in *Med1* KO molars at P7. **A**, mRNA expression for *Amel*, *Ambn*, *Enam*, *Mmp20*, *Alpl*, and *Calb1* in the dental epithelia derived from P7 molars of P7 CON and *Med1* KO mice evaluated by qPCR. The mRNA expression levels of each gene were normalized using the *Gapdh* mRNA expression levels. The normalized expression level of each gene in the CON mice was set as 1.0. Means  $\pm$  S.D. of relative expression are shown ( $n = 3$ ). Statistical significance is shown by *t* test (\*,  $p < 0.05$ ). **B**, immunostaining of AMEL, AMBN, and ALPL in P7 CON and *Med1* KO molars. The expression of AMEL, AMBN, and ALPL (green) and nuclear counterstaining with DAPI (blue) are shown. Enlarged images of the boxed (dotted line) areas in the left panels of the ALPL staining panel are shown in the right panels. H&E staining (HE panels) of equivalent sections is also shown in addition to the staining. Scale bars, 100  $\mu$ m (left panel) and 20  $\mu$ m (enlarged right panel). Arrowheads show ALPL-positive SI cells. *d*, dentin matrix; *e*, enamel matrix; *am*, ameloblast; *od*, odontoblast; *si*, stratum intermedium.

confirm the *in vivo* results that MED1 regulates Notch signaling and the expression of *Alpl*.

### *Med1* regulates SI differentiation and *Alpl* expression through Notch signaling

We next examined the involvement of Notch signaling in SI differentiation and *Alpl* expression using the  $\gamma$ -secretase inhibitor DAPT, which prevents the cleavage of NOTCH1 and thus inhibits Notch signaling. When the SF2 cells were

treated with DAPT, the levels of NICD were reduced in a dose-dependent manner with no change in NOTCH1 itself (Fig. 5A). In addition, DAPT reversed the MED1-induced *Alpl* and *Hes1* expression at the 96-h time point (Fig. 5B). To further confirm the involvement of Notch signaling in the *Alpl* induction, we transfected SF2 cells with the NICD expression vector, which mimics the action of NICD. The NICD transfection increased the expression of *Alpl* (Fig. 5C, left panel) and *Hes1* (Fig. 5C, right panel).

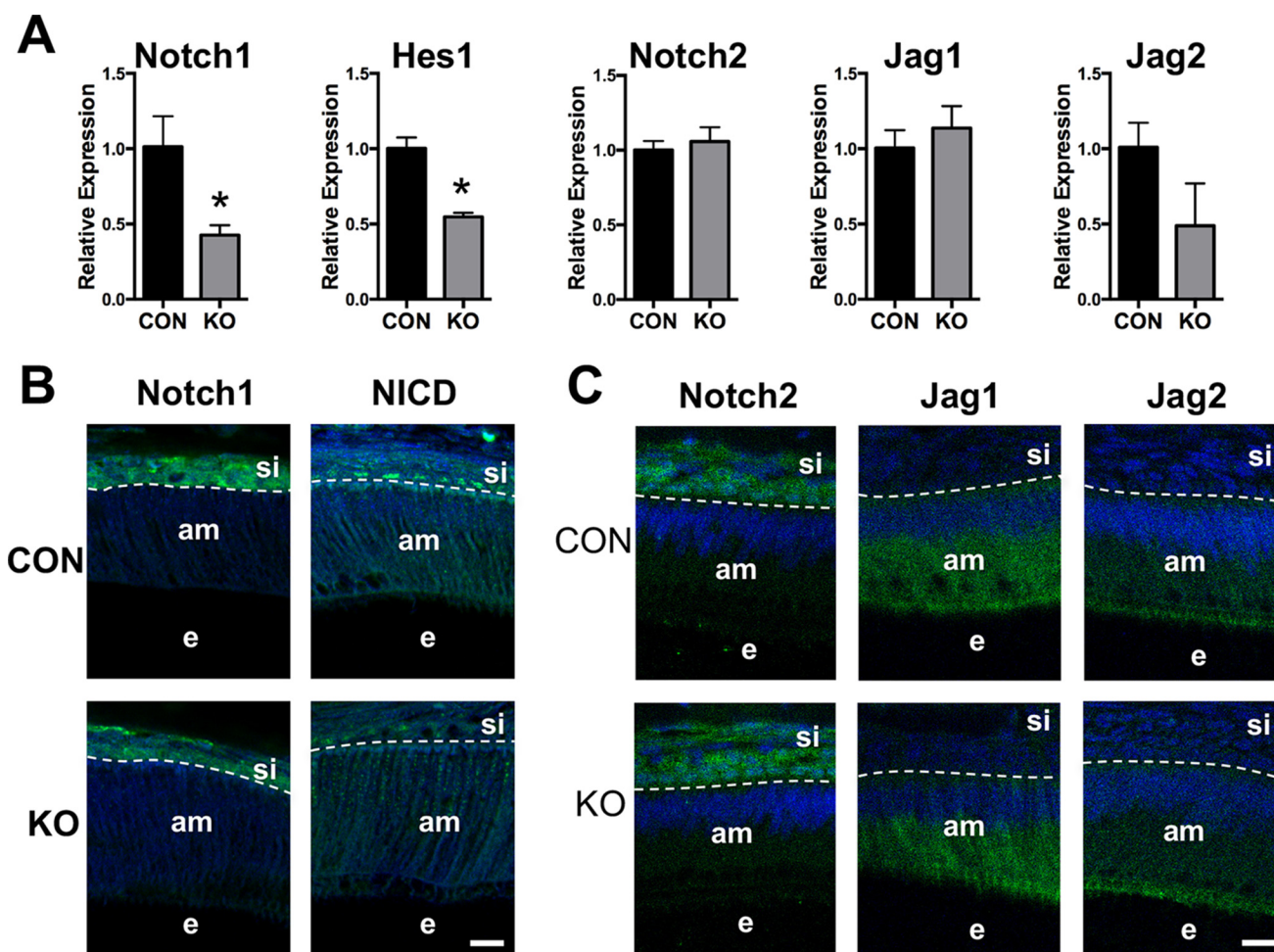


**Figure 3. Notch expression and signaling are down-regulated in Med1 KO dental epithelial cells at P7 molar.** A, expression levels of mRNA for *Notch1*, *Notch2*, *Hes1*, *Jag1*, and *Jag2* in dental epithelial tissues of *Med1* KO and CON P7 molars were evaluated by qPCR as described in the legend for Fig. 2. Means  $\pm$  S.D. of relative expression are shown ( $n = 3$ ). \*,  $p < 0.05$ . B and C, immunostaining of NOTCH1, NICD, JAG1, and JAG2 (green) in P7 CON and KO molars with DAPI counterstaining (blue). Scale bars, 10  $\mu$ m. e, enamel matrix; am, ameloblast; si, stratum intermedium cells.

**Med1 functions as a coactivator for Notch1 signaling to control gene transcription of *Alpl***

We examined whether MED1 was directly recruited into the promoter region of *Alpl* using chromatin immunoprecipitation (ChIP). *Med1*-overexpressing SF2 cells were fixed and immunoprecipitated with antibodies against MED1, RNA pol II, RBP-Jk, and IgG (control). The recruitment of MED1 and other proteins into the complex was detected by qPCR using primer sequences spanning the proximal region (site 1, -452 bp to -353 bp) containing the consensus DNA-binding sequences (GTGGGAA) for the RBP-Jk-binding site. The recruitment of MED1 into the distal region of the promoter lacking RBP-Jk (site 2, -2.5 to -2.4 kb) was also examined as a control. MED1, RBP-Jk, and RNA pol II were recruited into the proximal region of the *Alpl* promoter but not into the distal sites (Fig. 6A). When the cleavage of NOTCH1 was prevented by DAPT treatment, the recruitment of MED1 and pol II was inhibited, whereas the recruitment of RBP-Jk was not affected (Fig. 6, A and B, DAPT). These results suggest that MED1 is recruited into the RBP-Jk-binding site on the *Alpl* promoter only when NICD is present, whereas RBP-Jk does not require NICD for binding to this site. To confirm this proposition, we next examined whether MED1

directly interacts with NICD in the nucleus. Nuclear extracts were prepared from SF2 cells overexpressing MED1 and NICD, and transcriptional complexes were pulled down using antibodies against either MED1 or NICD (Fig. 6C). Both NICD and MED1 were detected in the MED1 pulldown complex, as compared with the IgG control (Fig. 6C, upper panels). Likewise, both NICD and MED1 were found in NOTCH1 complexes but not in the IgG control (Fig. 6C, lower panels). These results indicate that MED1 physically interacts with NICD in the nucleus. We next examined MED1 regulation of RBP-Jk transcriptional activity. The promoter reporter construct containing tandem repeats of the RBP-Jk-binding DNA sequence was transfected into SF2 cells, and transcriptional activity was evaluated by luciferase activity. SF2 cells showed basal RBP-Jk transcriptional activity after transfection with the reporter construct. When *Med1* was overexpressed, the RBP-Jk activity further increased (Fig. 6D). However, DAPT treatment abrogated both basal and *Med1*-induced transcriptional activity (Fig. 6D). These results indicated that MED1 facilitates the transcriptional activity of RBP-Jk through Notch signaling. We propose a model to show the MED1 regulation of *Alpl* transcription through Notch signaling (Fig. 6E). First of all, MED1

## Med1 activates alkaline phosphatase gene transcription

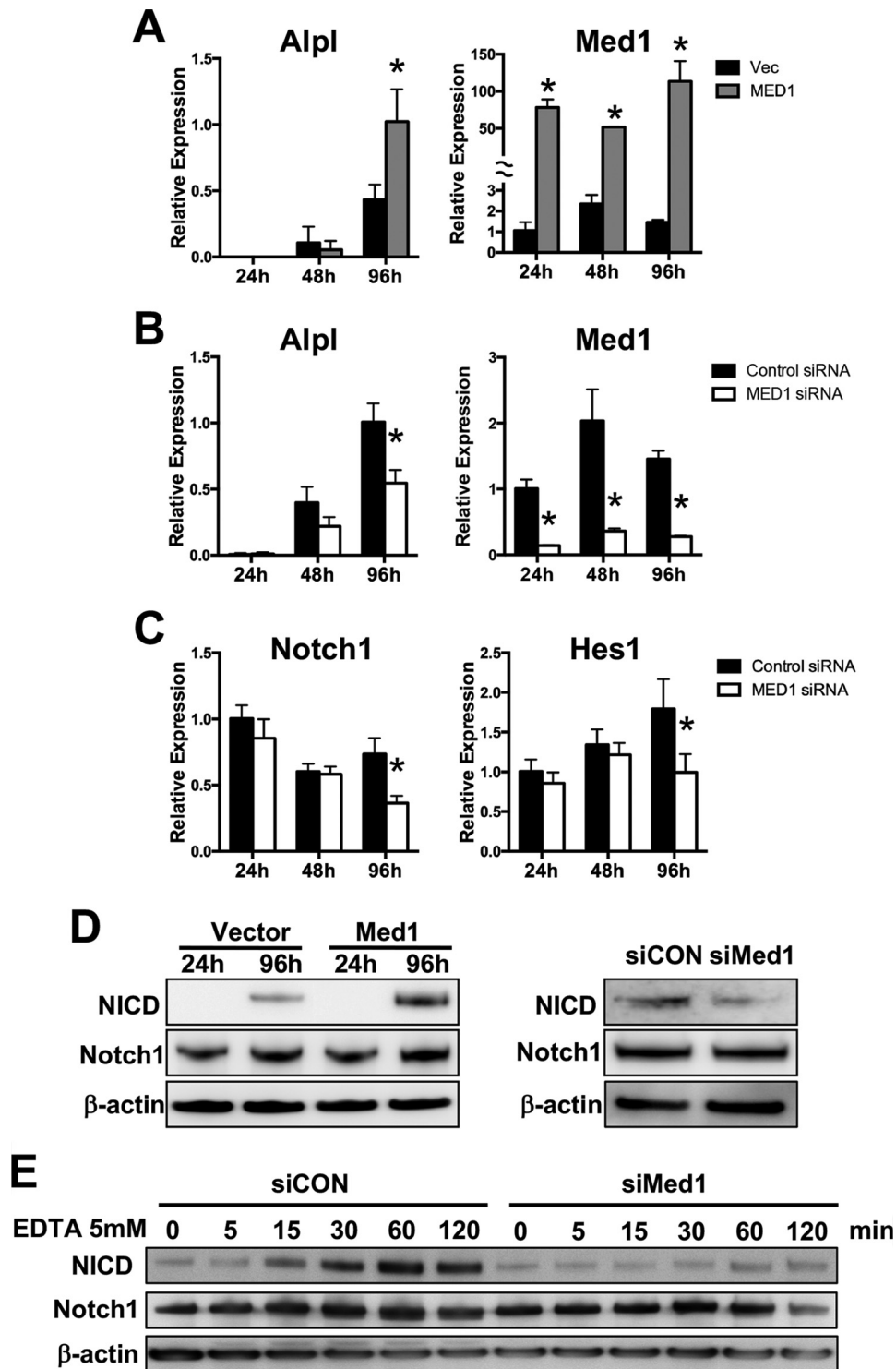


**Figure 4.** *Alpl* expression and Notch signaling are regulated by MED1 in SF2 cells. *A*, SF2 cells were transfected with mock vector (*Vec*) or *Med1* expression vector and maintained for 24–96 h. The mRNA levels of *Alpl* (left panel) and *Med1* (right panel) were monitored by qPCR. The *Alpl* mRNA expression levels were normalized using *Gapdh* mRNA expression levels. The normalized expression level of *Med1* in the CON mice at 24 h after transfection was set as 1.0. *B*, SF2 cells were transfected with siRNA for *Med1* (siMed1) or for control siRNA (siCON) and maintained for 24–96 h. *C*, mRNA levels for *Notch1* and *Hes1* on the same cells shown in *B*. *A–C*, data are shown as mean  $\pm$  S.D. ( $n = 3$ ). Statistical significance is shown by *t* test (\*,  $p < 0.05$ ). *D* and *E*, Western blotting for NICD and total NOTCH1 in the SF2 cells. *D*, cells were transfected with control vector or with *Med1* expression vector and maintained for 24 and 96 h (left panel), or cells were transfected with *Med1* siRNA or control siRNA for 72 h (right panel). *E*, the cells were transfected with *Med1* siRNA or control siRNA and treated with 5 mM EDTA for various time periods (0–120 min).  $\beta$ -Actin was used as an internal control.

stimulates the expression and activation of Notch1. In the activation of NOTCH1 signaling, the NICD is cleaved by specific proteases, such as  $\gamma$ -secretase, in either a ligand- or non-

ligand-dependent manner. The cleaved NOTCH1 is then translocated into the nucleus and binds to RBP-Jk on the *Alpl* promoter. MED1 then binds to NICD and forms a complex

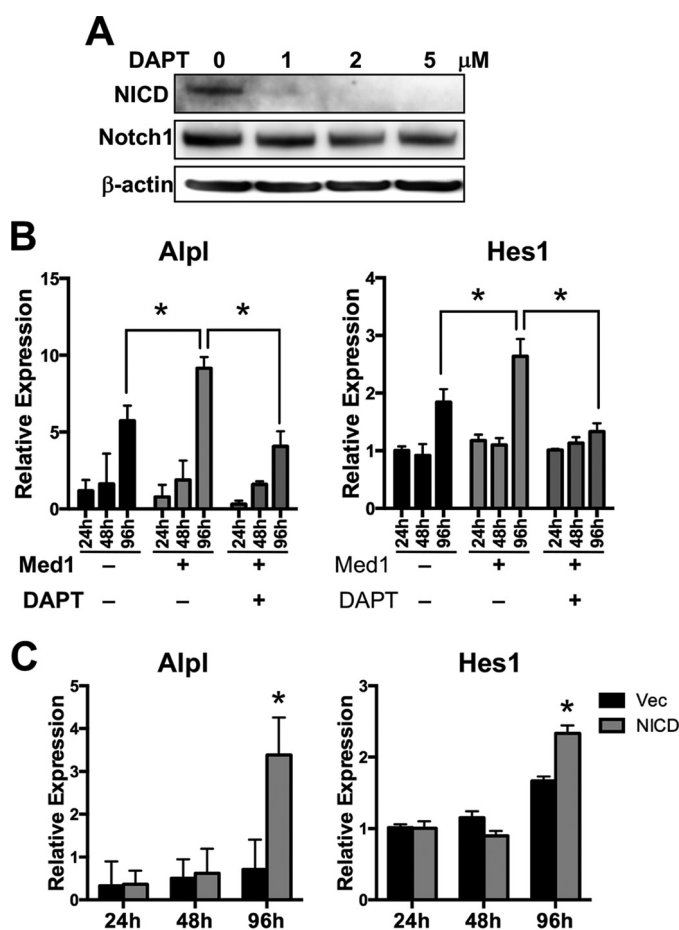


**Figure 5. Notch inhibitor DAPT decreases MED1-induced *Alpl* expression.** A, Western blotting of NICD, Notch1, and  $\beta$ -actin in SF2 cells that were treated with DAPT at different doses. B and C, mRNA levels of *Alpl* (left) and *Hes1* (right) were evaluated by qPCR. B, SF2 cells were transfected with mock vector or *Med1* expression vector. DAPT was added at 24 h after transfection and cells were maintained for 24–96 h. C, SF2 cells were transfected with mock vector (Vec) or NICD vector and maintained for 24–96 h. Mean  $\pm$  S.D. is shown ( $n = 3$ ) and statistical significance indicated (\*,  $p < 0.05$ ).

with RBP-Jk on the site 1 region of the *Alpl* promoter, which activates *Alpl* transcription by recruiting the transcription machinery including RNA pol II.

### Discussion

Previously, we reported that *Med1* deletion causes defects in incisor-specific stem cells that switch cell fate, resulting in ectopic hair generation and enamel defects in the incisor (24). This study demonstrated that *Med1* ablation causes enamel hypoplasia through not only defects in stem cell commitment but also through defects in Notch1-mediated SI differentiation. *Med1* ablation results in specific enamel defects in which the enamel matrix layer is formed but not mineralized. *Med1* deletion prevented the differentiation of SI but did not block commitment of dental epithelial stem cells to the IEE/ameloblast lineage. The matrix proteins were normally secreted and formed the enamel matrix layer in *Med1* KO molars, although Notch components and *Alpl* expression are reduced in the presumptive SI layer. These results suggest that *Med1* ablation may cause enamel hypomineralization through defects in *Alpl* expression during post-embryonic development. However, further studies are needed to prove

that MED1 is required for enamel mineralization directly through stimulation of *Alpl* gene transcription in SI cells.

We demonstrated that MED1 regulates gene transcription of *Alpl* *in vitro*, and this regulation was mediated through Notch signaling. We suggest that MED1 is essential for enamel mineralization through the regulation of *Alpl* in the SI layer at the secretory stage. MED1 may also function at the maturation stage in which SI cells are differentiated into the papillary layer cells and ALPL becomes involved in enamel matrix mineralization. However, MED1 may have other roles in the enamel mineralization process. *Med1* is also expressed in ameloblasts, especially at the maturation stage in the adult tooth, which may affect the enamel mineralization processes in *Med1* KO mice in addition to the *Alpl* expression defect in SI cells. Our previous study demonstrated that *Med1* deficiency disturbs the nuclear polarization of ameloblasts and reduced gene expression at the maturation stage of adult incisors (24).

As noted above, we demonstrated that MED1 regulates enamel mineralization and Notch signaling. However, a recent study shows that Mediator regulates cell-specific gene transcription by forming a super-enhancer in which several different fate transcription factors are recruited to induce lineage-specific transcription (16). Therefore, it is still possible that MED1 regulates other signal pathways or transcription factors required for enamel mineralization together with Notch signaling.

We also demonstrated that MED1 regulates Notch1 signaling through transcriptional regulation. However, the expression of NOTCH1 and NICD was reduced in *Med1* KO molars (P7) as well as in *Med1*-silenced SF2 cells. MED1 also may influence the activation of NOTCH1 by regulating  $\gamma$ -secretase, which cleaves NOTCH1 to activate Notch signaling. In fact, our preliminary results showed that components of  $\gamma$ -secretase are down-regulated in siMed1 cells (data not shown).

Taken together, our *in vivo* and *in vitro* results suggest that MED1 facilitates enamel mineralization through the regulation of Notch1-mediated *Alpl* expression in SI cells. ALPL is critical for mineralization in bone and tooth (3, 4). The tissue-nonspecific ALPL promotes extracellular matrix mineralization by increasing the local availability of phosphate needed for hydroxyapatite crystal formation in bone and tooth.

MED1 acts as a coactivator for Notch1 signaling and directly regulates the transcription of *Alpl*. MED1 is specifically recruited into the RBP-Jk-binding site of the *Alpl* promoter, indicating that MED1 controls Notch1 transcriptional activity.

Our results indicate that MED1 has a critical role in the mineralization of enamel through *Alpl*. *Krt14*-specific *Med1* KO mice did not show defects in dentin and bone, as these tissues do not have *Krt14*-expressing epithelia, although *Med1* is expressed in osteoblasts, odontoblasts, and dental mesenchyme cells in teeth (data not shown). The specific deletion of *Med1* from these cells may reveal a role for MED1 in mineralization in these tissues as well.

In summary, our results reveal that MED1 functions as a coactivator for Notch signaling and directly regulates gene transcription of *Alpl* in tooth enamel organ. *Alpl* expression in the SI appears to be necessary for enamel matrix mineralization during tooth development. This observation suggests a role for the SI cells in enamel matrix mineralization that has not been explored previously.



## Med1 activates alkaline phosphatase gene transcription

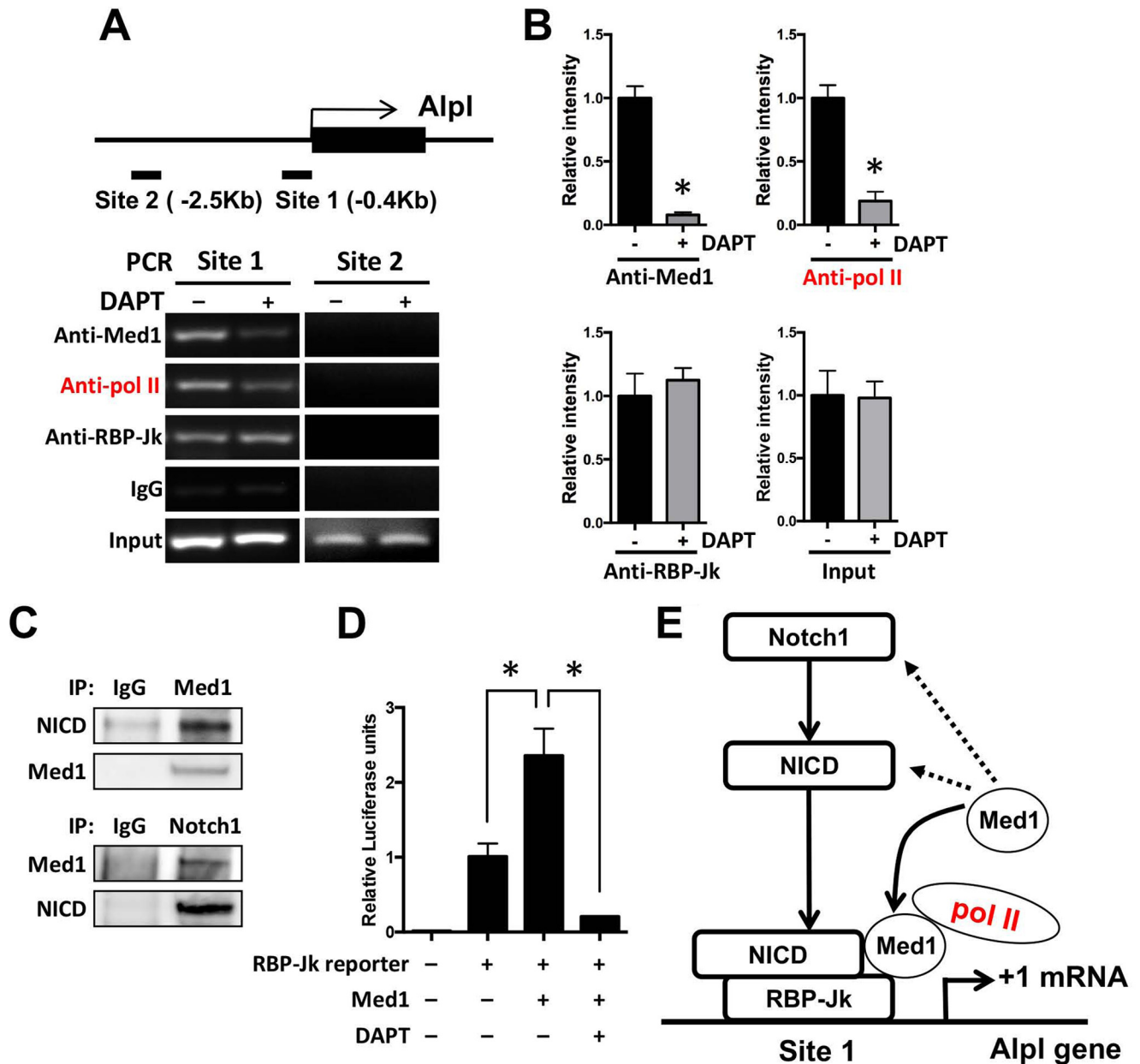


**Figure 6. MED1 binds to NICD and acts as a coactivator of NICD/RBP-Jk for *Alpl* transcription in SF2 cells.** *A*, ChIP assays using antibodies to MED1, RNA pol II, RBP-Jk, and IgG. Nuclear extracts were prepared from *Med1*-transfected SF2 cells with or without DAPT treatment. The extracts were immunoprecipitated with the appropriate antibodies. Genomic PCR was performed using primer sets for site 1 (-452 bp to -353 bp) and site 2 (-2.4 kbp to -2.5 kbp) in the *Alpl* promoter. *B*, quantitation of the PCR bands shows the incorporation of MED1, RNA pol II, and RBP-Jk into site 1. Mean  $\pm$  S.D. ( $n = 3$ ) and statistical significance are shown.  $^*p < 0.05$ . *C*, MED1 and NICD interaction by immunoprecipitation (IP) analysis. SF2 cells were transfected with *Med1* and NICD expression vectors. The cell lysates were immunoprecipitated by antibodies for either MED1 (upper panel) or NOTCH1 (lower panel). The incorporation of MED1 and NICD was detected by Western blotting using antibodies against MED1 or NICD. *D*, RBP-Jk promoter reporter activity was evaluated in SF2 cells transfected with *Med1* expression vector with and without DAPT. DAPT was added 24 h after transfection. The luciferase activity in RBP-Jk reporter-transfected SF2 cells was set as 1. Mean  $\pm$  S.D. is shown ( $n = 3$ ).  $^*p < 0.05$ . *E*, schematic diagram of MED1-mediated activation of *Alpl* transcription through Notch1 signaling in SF2 cells. Direct and indirect points of regulation are shown by solid and dotted lines, respectively.

## Experimental procedures

### Mouse model of *Med1* conditional KO mice

To delete the expression of *Med1* in dental epithelial cells, floxed *Med1*-mice were mated with *Krt14Cre* mice as described previously (23). Floxed *Med1* mice with the *Krt14Cre* transgene (*Med1* KO) and control floxed *Med1* mice without *Krt14-Cre* (CON) were used for this study. Genotyping was performed by PCR as described previously (23). All of the experiments were

approved by the Institutional Animal Care and Ethics Committee at the San Francisco Department of the Veterans Affairs Medical Center.

### Tissue preparation, histological analysis, and immunostaining

The heads of postnatal day 7 (P7) and 10-week-old control and *Med1* KO mice were excised and fixed with 4% paraformaldehyde in PBS overnight at 4 °C. For histological and immuno-

**Table 1**  
Primer sequences for quantitative RT-qPCR

Gene name	Forward primer	Reverse primer
<i>Med1</i>	5'-ctccaatccttagaacag-3'	5'-gataaccaacacttccat-3'
<i>Ambn</i>	5'-gcgtttccaagagccctgataac-3'	5'-aagaagcagtggtcacatttctctgg-3'
<i>Amel</i>	5'-attccaccccagtcctcatcagc-3'	5'-ttcttcccgttggctctgtc-3'
<i>Enam</i>	5'-gtfctcctgttttctcctgggtctg-3'	5'-tttggcggtctcctgggttcttc-3'
<i>Mmp20</i>	5'-caatttattcaccggtgtgctg-3'	5'-ggtcctgataatgcttggat-3'
<i>Alpl</i>	5'-agagcttcaaacctagac-3'	5'-gttccgattcaactcatac-3'
<i>Calb1</i>	5'-cagtcactctctgatcaca-3'	5'-ctcctggatcaagttctg-3'
<i>Notch1</i>	5'-aataagaggacaagaatt-3'	5'-gaagcaatcaataaataaac-3'
<i>Notch2</i>	5'-gaggatgaggcttctgctgc-3'	5'-gttctgcctgaggaggagtg-3'
<i>Hes1</i>	5'-tcttctgacggacactaa-3'	5'-cgcaatccaatatgaacat-3'
<i>Jag2</i>	5'-aaggcctgtgcatagtt-3'	5'-atccgagaatactccgttgtt-3'
<i>Gapdh</i>	5'-ggagcgagaccacctaacatc-3'	5'-ctcgtggttcacaccatcac-3'

histochemical analyses, P7 heads were decalcified with 250 mM EDTA/PBS for 7 days and processed for embedding in paraffin. Next, 8- $\mu$ m sections were sliced using a microtome. The sections were stained with Harris hematoxylin (Sigma-Aldrich) and eosin Y (Sigma-Aldrich) for a detailed morphological analysis of the incisors. For immunohistochemistry, sections were dehydrated, rehydrated, and then pretreated in 10 mmol/liter citrate buffer, pH 6.0 (Sigma-Aldrich), for 20 min using a microwave for antigen retrieval. The specimens were blocked using Power Block (BioGenex) and reacted with primary antibodies to ALPL (R&D System), NOTCH1, NOTCH2, NICD, JAG1, and JAG2 (Cell Signaling), AMBN (Santa Cruz Biotechnology), and AMEL (Abcam) overnight at 4 °C. Primary antibodies were detected using Alexa Fluor 488 (Invitrogen). Nuclear staining was performed with DAPI (Sigma-Aldrich). Immunostaining analysis was performed using a LSM 510 inverted confocal microscope (Carl Zeiss).

### Scanning electron microscopy

Incisors of 10-week-old CON and *Med1* KO mice were dissected. The specimens were embedded in epoxy resin, cut with an IsoMet low-speed saw, treated with 40% phosphoric acid for 10 s and then with 10% sodium hypochlorite for 30 s, coated with gold, and photographed using electron microscopy at 20 kV (S-3500, Hitachi Ltd.).

### Cell culture and transfection

The dental epithelial cell line SF2 (26, 27) was maintained in DMEM/F-12 (Invitrogen) supplemented with 10% FBS (HyClone) and 1% penicillin and streptomycin at 37 °C in a humidified atmosphere containing 5% CO<sub>2</sub>. To transfect the expression vectors for *Med1* and constitutively activate Notch (NICD) and siRNA for *Med1*, SF2 cells were plated in 12-well plates at a density of 4 × 10<sup>5</sup> cells/ml/well. The cells were transfected using Lipofectamine LTX (Invitrogen) for expression vectors and Lipofectamine RNAiMAX (Invitrogen) for siRNA according to the manufacturer's protocol. To inhibit the Notch signaling pathway, 2  $\mu$ M DAPT, a  $\gamma$ -secretase inhibitor (Sigma-Aldrich), was added to the cells.

### Western blotting

SF2 cells were washed with PBS and then solubilized in 100  $\mu$ l of CellLytic M cell lysis reagent (Sigma-Aldrich) containing protease inhibitor mixture tablets (cOMplete Mini, Roche). Lysed cells were then centrifuged at 12,000 rpm for 30 min at

4 °C, and the supernatant was collected. The protein concentration was measured using Micro-BCA assay reagent (Thermo Fisher Scientific). Next, a 10- $\mu$ g sample of each protein was electrophoresed on a 4–12% SDS-polyacrylamide gel (Invitrogen) and transferred to a PVDF filter membrane (Invitrogen). The blotted membrane was incubated with antibodies against MED1 (Santa Cruz Biotechnology),  $\beta$ -actin (Abcam), NICD (Cell Signaling), and NOTCH1 (Cell Signaling). Signals were detected with an ECL kit (Thermo Fisher Scientific).

### RNA isolation and RT-qPCR

The molars from P7 *Med1* KO and CON mice were dissected. Epithelial tissues were separated from the P7 molars under a microscope. Total RNA was isolated using TRIzol (Invitrogen) according to the manufacturer's protocol. Total RNA (1  $\mu$ g) was used for reverse transcription to generate cDNA. First-strand cDNA was synthesized at 42 °C for 60 min using random primers with SuperScript III (Invitrogen). PCR amplification was performed using the primers listed in Table 1. Real-time qPCR was performed with iQ SYBR Green Supermix (Bio-Rad Laboratories) and a CFX96 thermal cycler (Bio-Rad Laboratories). Gene expression was normalized to the housekeeping gene *Gapdh* in each sample.

### Immunoprecipitation (IP) Assay

SF2 cells were plated in 60-mm dishes at a density of 2 × 10<sup>6</sup> cells in 3 ml of the media/dish and then transfected with the *Med1* and NICD expression vectors for 24 h. The cells were then harvested for nuclear extraction using a nuclear extract kit (Active Motif). The nuclear fraction was analyzed using an immunoprecipitation kit (Invitrogen). Antibodies against MED1, NICD, and control IgG were fused with protein G-magnetic beads and incubated in the nuclear fraction (100  $\mu$ g/500  $\mu$ l) for 4 h at 4 °C. The complex was eluted and denatured by NuPAGE LDS sample buffer (Invitrogen) with 1% 2-mercaptoethanol. The samples were analyzed by Western blotting.

### Luciferase assay

The RBP-Jk activity was analyzed using a Cignal RBP-Jk reporter (luc) kit (Qiagen). The RBP-Jk reporter plasmid was transfected into SF2 cells either with mock vector or the *Med1* expression vector. Activity was determined 48 h later with the Dual-Luciferase reporter assay system (Promega) using a luminometer (Berthold). The firefly luciferase activity was normalized for *Renilla* luciferase activity as an internal control.

# Med1 activates alkaline phosphatase gene transcription

## Chromatin immunoprecipitation assay

To examine whether MED1 interacts directly with the promoter region of *Alpl*, ChIP assays were performed in SF2 cells either with or without DAPT using a ChIP-IT express kit (Active Motif) according to the manufacturer's protocol. Cross-linked chromatin lysates were sonicated, incubated with antibodies against MED1 (Santa Cruz Biotechnology), RNA pol II (Active Motif), RBP-Jk (Santa Cruz Biotechnology), and control IgG (Active Motif) at 4 °C overnight, and then precipitated with protein G–magnet beads. Cross-linking was reversed using a reverse cross-linking buffer, and DNA fragments were analyzed by PCR using the following primer pairs, specific for their respective promoter region, on an agarose gel. For the *Alpl* promoter site1, the forward primer used was TCTGCTTCCTACTGACTT, and the reverse primer was ACATCCTTGTCTGTAACC. For the *Alpl* promoter site 2, the forward primer was AGTCTTATTGTGCTTATTGT and the reverse primer was AGTTGTGAAAGGAAAGTC.

## Statistical analysis

All of the experiments in this study were repeated at least three times, and reproducibility was confirmed. The data were analyzed using Prism 6 software (GraphPad Software Inc.), and  $p < 0.05$  was considered statistically significant.

**Author contributions**—K. Y. designed the study, performed the experiments and the data analysis, and wrote the manuscript. L. H., T. N., K. S., M. I., I. T., and S. F. contributed in conducting the experiments and the data analysis. Y. O., L. H., T. N., and D. D. B. generated and bred the transgenic mice. Y. O., D. D. B. P. D., and Y. Y. initiated and designed the study, performed the data analysis, and prepared the manuscript. All authors reviewed the results and approved the final version of the manuscript.

## References

1. Yoshizaki, K., and Yamada, Y. (2013) Gene evolution and functions of extracellular matrix proteins in teeth. *Orthod. Waves* **72**, 1–10
2. Fukumoto, S., and Yamada, Y. (2005) Review: Extracellular matrix regulates tooth morphogenesis. *Connect Tissue Res.* **46**, 220–226
3. Gasque, K. C., Foster, B. L., Kuss, P., Yadav, M. C., Liu, J., Kiffer-Moreira, T., van Elsas, A., Hatch, N., Somerman, M. J., and Millán, J. L. (2015) Improvement of the skeletal and dental hypophosphatasia phenotype in *Alpl*<sup>-/-</sup> mice by administration of soluble (non-targeted) chimeric alkaline phosphatase. *Bone* **72**, 137–147
4. McKee, M. D., Yadav, M. C., Foster, B. L., Somerman, M. J., Farquharson, C., and Millán, J. L. (2013) Compounded PHOSPHO1/ALPL deficiencies reduce dentin mineralization. *J. Dent. Res.* **92**, 721–727
5. Kawano, S., Saito, M., Handa, K., Morotomi, T., Toyono, T., Seta, Y., Nakamura, N., Uchida, T., Toyoshima, K., Ohishi, M., and Harada, H. (2004) Characterization of dental epithelial progenitor cells derived from cervical-loop epithelium in a rat lower incisor. *J. Dent. Res.* **83**, 129–133
6. Yadav, M. C., de Oliveira, R. C., Foster, B. L., Fong, H., Cory, E., Narisawa, S., Sah, R. L., Somerman, M., Whyte, M. P., and Millán, J. L. (2012) Enzyme replacement prevents enamel defects in hypophosphatasia mice. *J. Bone Miner. Res.* **27**, 1722–1734
7. Cai, X., Gong, P., Huang, Y., and Lin, Y. (2011) Notch signalling pathway in tooth development and adult dental cells. *Cell Prolif.* **44**, 495–507
8. Harada, H., Ichimori, Y., Yokohama-Tamaki, T., Ohshima, H., Kawano, S., Katsube, K., and Wakisaka, S. (2006) Stratum intermedium lineage diverges from ameloblast lineage via Notch signaling. *Biochem. Biophys. Res. Commun.* **340**, 611–616
9. Mitsiadis, T. A., Graf, D., Luder, H., Gridley, T., and Bluteau, G. (2010) BMPs and FGFRs target Notch signalling via jagged 2 to regulate tooth morphogenesis and cytodifferentiation. *Development* **137**, 3025–3035
10. Rand, M. D., Grimm, L. M., Artavanis-Tsakonas, S., Patriub, V., Blacklow, S. C., Sklar, J., and Aster, J. C. (2000) Calcium depletion dissociates and activates heterodimeric notch receptors. *Mol. Cell. Biol.* **20**, 1825–1835
11. Blazek, E., Mittler, G., and Meisterernst, M. (2005) The mediator of RNA polymerase II. *Chromosoma* **113**, 399–408
12. Bourbon, H. M., Aguilera, A., Ansari, A. Z., Asturias, F. J., Berk, A. J., Bjorklund, S., Blackwell, T. K., Borggreffe, T., Carey, M., Carlson, M., Conaway, J. W., Conaway, R. C., Emmons, S. W., Fondell, J. D., Freedman, L. P., et al. (2004) A unified nomenclature for protein subunits of mediator complexes linking transcriptional regulators to RNA polymerase II. *Mol. Cell* **14**, 553–557
13. Kornberg, R. D. (2005) Mediator and the mechanism of transcriptional activation. *Trends Biochem. Sci.* **30**, 235–239
14. Malik, S., and Roeder, R. G. (2005) Dynamic regulation of pol II transcription by the mammalian Mediator complex. *Trends Biochem. Sci.* **30**, 256–263
15. Kagey, M. H., Newman, J. J., Bilodeau, S., Zhan, Y., Orlando, D. A., van Berkum, N. L., Ebmeier, C. C., Goossens, J., Rahl, P. B., Levine, S. S., Taatjes, D. J., Dekker, J., and Young, R. A. (2010) Mediator and cohesin connect gene expression and chromatin architecture. *Nature* **467**, 430–435
16. Whyte, W. A., Orlando, D. A., Hnisz, D., Abraham, B. J., Lin, C. Y., Kagey, M. H., Rahl, P. B., Lee, T. I., and Young, R. A. (2013) Master transcription factors and mediator establish super-enhancers at key cell identity genes. *Cell* **153**, 307–319
17. Yue, X., Izcue, A., and Borggreffe, T. (2011) Essential role of Mediator subunit Med1 in invariant natural killer T-cell development. *Proc. Natl. Acad. Sci. U.S.A.* **108**, 17105–17110
18. Stumpf, M., Yue, X., Schmitz, S., Luche, H., Reddy, J. K., and Borggreffe, T. (2010) Specific erythroid-lineage defect in mice conditionally deficient for Mediator subunit Med1. *Proc. Natl. Acad. Sci. U.S.A.* **107**, 21541–21546
19. Jiang, Q., Hu, Q., Ito, M., Meyer, S., Waltz, S., Khan, S., Roeder, R. G., and Zhang, X. (2010) Key roles for MED1 LxxLL motifs in pubertal mammary gland development and luminal-cell differentiation. *Proc. Natl. Acad. Sci. U.S.A.* **107**, 6765–6770
20. Jia, Y., Qi, C., Zhang, Z., Zhu, Y. T., Rao, S. M., and Zhu, Y. J. (2005) Peroxisome proliferator-activated receptor-binding protein null mutation results in defective mammary gland development. *J. Biol. Chem.* **280**, 10766–10773
21. Oda, Y., Chalkley, R. J., Burlingame, A. L., and Bikle, D. D. (2010) The transcriptional coactivator DRIP/Mediator complex is involved in vitamin D receptor function and regulates keratinocyte proliferation and differentiation. *J. Invest. Dermatol.* **130**, 2377–2388
22. Bikle, D., Teichert, A., Hawker, N., Xie, Z., and Oda, Y. (2007) Sequential regulation of keratinocyte differentiation by 1,25(OH)2D3, VDR, and its coregulators. *J. Steroid Biochem. Mol. Biol.* **103**, 396–404
23. Oda, Y., Hu, L., Bul, V., Elalieh, H., Reddy, J. K., and Bikle, D. D. (2012) Coactivator MED1 ablation in keratinocytes results in hair-cycling defects and epidermal alterations. *J. Invest. Dermatol.* **132**, 1075–1083
24. Yoshizaki, K., Hu, L., Nguyen, T., Sakai, K., He, B., Fong, C., Yamada, Y., Bikle, D. D., and Oda, Y. (2014) Ablation of coactivator Med1 switches the cell fate of dental epithelia to that generating hair. *PLoS ONE* **9**, e99991
25. Nakamura, T., de Vega, S., Fukumoto, S., Jimenez, L., Unda, F., and Yamada, Y. (2008) Transcription factor epiprofin is essential for tooth morphogenesis by regulating epithelial cell fate and tooth number. *J. Biol. Chem.* **283**, 4825–4833
26. Arakaki, M., Ishikawa, M., Nakamura, T., Iwamoto, T., Yamada, A., Fukumoto, E., Saito, M., Otsu, K., Harada, H., Yamada, Y., and Fukumoto, S. (2012) Role of epithelial-stem cell interactions during dental cell differentiation. *J. Biol. Chem.* **287**, 10590–10601
27. Dassule, H. R., Lewis, P., Bei, M., Maas, R., and McMahon, A. P. (2000) Sonic hedgehog regulates growth and morphogenesis of the tooth. *Development* **127**, 4775–4785